

OXIDIC SHIELD AND ITS INFLUENCE ON THE REACTIVITY AND MIGRATION OF AIR-STABLE IRON NANOPARTICLES

PEŠKOVÁ Kristýna, ČERNÍK Miroslav, RIBAS David, BENITO José, MARTI Vicens, PARMA Petr, LACINOVA Lenka, ZBOŘIL Radek, FILIP Jan

Technical University of Liberec, Liberec, Czech Republic, EU

Abstract

Nanoscale Zero Valent Iron (nZVI) can be protected from rapid oxidation by various methods including the use of organic or inorganic molecules. A simple oxide layer allows long-term storage of nZVI on contact with air, as well as safe delivery and simple manipulation. On the other hand, the protection is so good that simple dilution in water cannot deactivate the protective layer and the nanoparticles must be activated prior to their application. The activation process involves preparing concentrated nZVI/water slurry (20% wt.) and leaving it for 48 hours. In the present research, three types of particles with different oxide shell thicknesses were compared in order to assess their reactivity with Cr(VI) as a representative contaminant. The results showed a diminution in the reduction capacity of Cr(VI) with increasing shell thickness. The activation process was able to create irregularities in the protective oxide shell with a thickness of <3.4 nm and to significantly improve Cr(VI) reduction.

Keywords: nZVI, nanoiron, reductive processes, remediation

1. INTRODUCTION

The presented research is performed in the framework of the EU FP7 project entitled NANOREM "Taking Nanotechnological Remediation Processes from Lab Scale to End User Applications for the Restoration of a Clean Environment", which aims to develop new types of iron nanoparticles for the remediation of the groundwater. The nanoparticles should be air-stable but not require storage in an inert atmosphere or as water slurry. This greatly simplifies the handling of the material prior to remediation (transport and storability). The pyrophoric properties of the original nanoparticles are suppressed by stabilizing their surface with an inorganic shell, which prevents rapid oxidation on contact with air. The characteristics show that such a layer has a thickness of a single nm and has no influence on the Fe⁰ content. Laboratory tests show that the reactivity of the particles and their ability to migrate are negatively affected by the thickness of the oxide shell. Due to a gradual breakdown of the inorganic oxide shell and the subsequent exposure of the reactive surface to air, stable nZVI particles demonstrate a delay in the onset of the reactivity and their capacity is lowered as well. The present work describes a new method for recovering the reactivity of nZVI particles protected by an oxide layer and to enhance their properties. Three types of nZVI particles with different oxide shell thicknesses were tested for their reactivity and migration properties before and after the activation process. The nanoparticles with the thinnest oxide layer and activated in water show the best reactivity and migration.

2. MATERIALS TESTED

Zero-valent iron nanoparticles with different oxide layer thicknesses, named STAR 400 and STAR 197, were compared with commercial NANOFER 25P (hereafter referred to as 25P). The STAR particles are air-stable because their surface is stabilized by an oxide layer; unlike 25P particles, which are pyrophoric because they have no tailored surface modification leading to rapid oxidation on contact with air (flammable iron). Suspensions of 25P were prepared from powdered products in distilled water with a ratio of 1: 4 (20% water slurry) using an LD 05 laboratory dispersing unit (Nanolron s.r.o.) in a nitrogen atmosphere immediately prior to application. Similarly, the STAR suspensions were prepared as 20% water slurry dispersed with a

homogenizing and dispersing device (MICCRA D-9 ART Prozess & Labortechnik GmbH & Co. KG) at 11,000 rpm for two minutes. To recover the reactive surface of the iron particles prior to their application, a simple activation process was investigated. The 20% nZVI slurry was aged for 48 hours at room temperature without any additional shaking. After 2 days the activated nZVI slurry was dispersed for two minutes as it is done for the slurry preparation. The storage solution can then be diluted to the final concentration for subsequent experiments.

3. LABORATORY TEST METHODOLOGIES

Batch experiments

Batch tests with a model contaminant (hexavalent chromium) were designed to determine the reactivity of the nZVI samples in activated and unactivated states. The reactivity tests with Cr(VI) (initial concentration of 50 mg/L) were performed in 100 hermetically closed bottles with different amounts of nZVI to obtain a final concentration of 0.1, 0.25, 0.5, 2.0, 2.5, 4.0 and 8.0 g/L. The solution was left to react for 24 hours with a bottom-up rotation every 60 s to avoid particle settling. The decrease in the concentration of Cr(VI) and changes in the pH and ORP were monitored using a spectrophotometer (DR3900) and multimeter (WTW 343i), respectively. The 24 h reaction time was chosen since the preliminary batch tests showed that Cr(VI) depletion took place mainly within the first 2 h.

The reactivity tests with chlorinated hydrocarbons (CHCs) were carried out with real polluted water from an industrial site. The tests were carried out in 250 ml glass reagent bottles with a Teflon septum. To prevent volatilization, the sample containers were prepared separately for each measured time. In this case the tests were performed only with STAR 197 (concentration of 2 g/L) with or without activation. The sample was placed in a vertical revolving shaker and subsequently analyzed at specific times for CHC content by GC/MS (Varian 3800/Saturn 2800), pH and ORP (WTW 343i). The natural rate of volatilization of the sample was evaluated based on analysis of the control samples without nZVI.

Column experiments

For the column tests, a 2 m long column with an inner diameter of 2.5 cm was used. The column has a vertical orientation and was washing against the direction of gravity. The column was filled with sand with a grain size smaller than 1 mm. A funnel was used to fill the column as homogeneously as possible and the sand was compacted by vibrating. In order to reduce the oxidation processes the column was flushed with nitrogen and saturated with degassed water. Washing of the column was provided by two peristaltic pumps: a circulation pump (PCD825, Čerpadla Kouřil) providing the main water flow in the system (the water also passes through a MAD-02 degasser, REGOM INSTRUMENTS s.r.o.) and a dosing pump (PCD21, Čerpadla Kouřil) for continuous dosing of the aqueous nZVI suspension from a stirred tank, which was purged with argon to suppress the oxidation of nZVI. The concentration used for the experiment was 10 g/L. The concentration of iron in the column was monitored through measurement of magnetic susceptibility, which is significantly higher for zero-valent iron than for cationic forms. A scanner was specially designed for this measurement. Every 10 minutes the column was scanned and the content of nZVI was evaluated. The pressure was also monitored on the input of the column.

Nanoparticle characterization by electron microscopy

For electron microscopy characterization, the samples were prepared in a glove box in a nitrogen atmosphere with air locks (Jacomex 2P) keeping the oxygen concentration below 5 ppm. The samples were suspended by mixing vigorously in absolute ethanol. For the SEM studies (Gemini ultra plus, Zeiss) the samples were deposited and led to evaporate over standard pins. For the TEM studies (Philips CM30, operating at 300 kV) a droplet was placed on a 300 copper mesh grid with a supporting film made of holey carbon (Agar Scientific, S147-3). Pyrophoric samples were transferred to the microscope in a liquid nitrogen flask to reduce contact with oxygen. Detailed nZVI surface observation was performed using a HRTEM (TITAN) operating at 300 kV.

4. RESULTS

The TEM images of the unactivated (UA) and activated (A) nZVI samples were used to determine the thickness of the oxide layer (**Fig. 1**). For UA 25P nanoparticles, a uniform and thin oxide layer around 1.8 nm thick was observed. The oxide stabilization process produces a uniform layer with significantly a thicker oxide layer of 3.4 nm for UA STAR 197 and 6.5 nm for UA STAR 400, respectively. The activated nanoparticles (A 25P) only displayed minor changes, except perhaps for the fact that the oxide layer appeared to be slightly more distorted with some detached oxides accumulated in zones in the outer shell. However, substantial changes in the oxide shell morphology were found for A STAR 197 nanoparticles. The surface revealed numerous irregularities caused by the dissolution and loss of large shell zones. In the case of A STAR 400, the nanoparticles still contained a uniform oxide shell with just a few discontinuities, but with a clear reduction in their thickness.

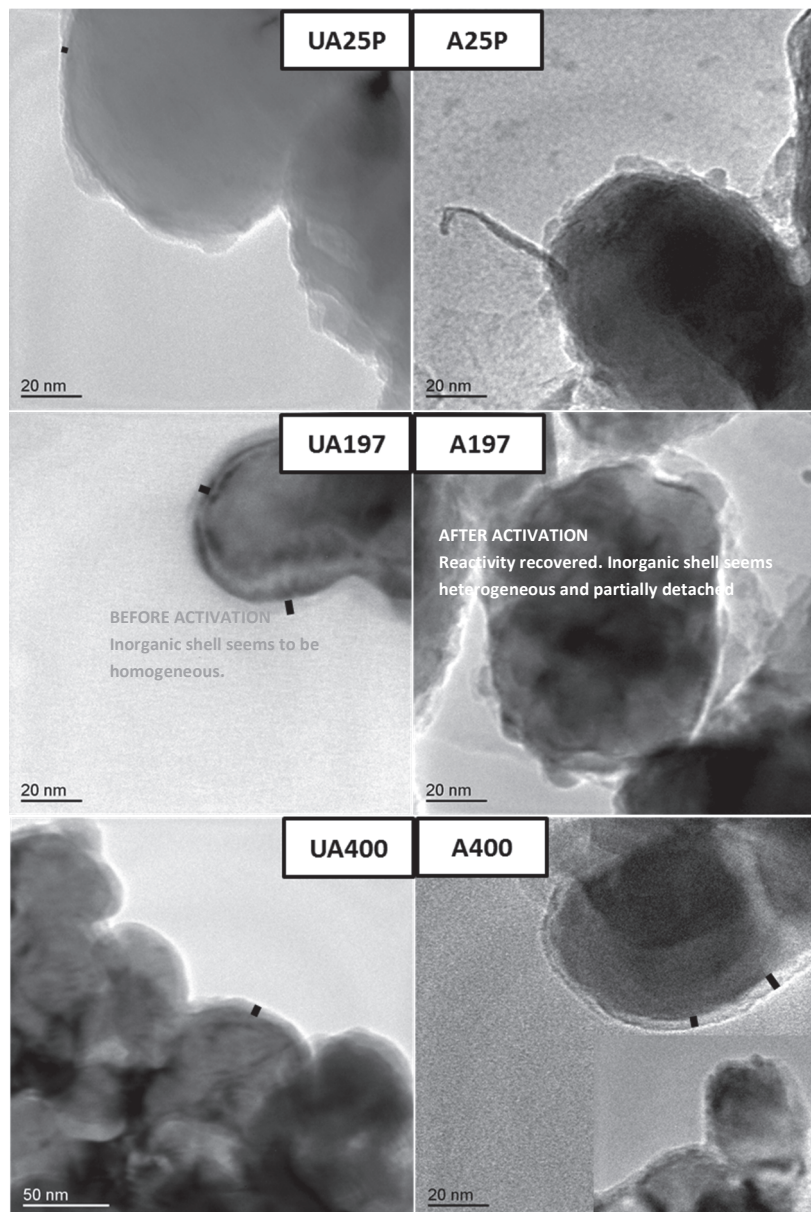


Fig. 1 TEM images of the three types of nanoparticles before and after activation

The changes in the Fe(0) content during the activation process are insignificant, which is consistent with the low presence of aging oxides in the TEM observation (**Table 1**). In other cases, highly concentrated slurries (200 ZVI g/l) with or without a very low stirring speed together with a high pH have shown a very similar behaviour (Sarathy, 2008; Liu 2006). In contrast, if the slurries had a low concentration, low pH, significant

stirring speed or a significant presence of oxygen, the loss of Fe(0) was dramatic at similar aging times (Kim 2010; Xie 2012, Liu and Zhang 2014, Liu 2015). These results are very relevant since they indicate that the nZVI was not sacrificed during the activation process.

Table 1 Zero valent iron content of the tested irons before and after activation

% wt	NF 25P	NF STAR 197	NF STAR 400
UA	87±1	78±1	50±1
A	86±1	77±1	50±1

Batch tests

The concentration trends of Cr(VI) as a function of the nZVI concentration for the studied nanoparticles are shown in **Fig. 2**. As it can be seen, the Cr(VI) removal was linearly proportional to the amount of nZVI applied. The slope varied with the type of nZVI and depended on the activation process. The highest reactivity of 25P nanoparticles revealed very little differences between the activated and the unactivated state. On the contrary, the surface stabilized nanoparticles in the unactivated state, UA STAR 197 and 400, showed very low reactivity compared to NF 25P. However, once activated, these nanoparticles experienced a significant improvement in reactivity. In the case of A STAR 197, the removal capacity of Cr(VI) increased nearly five times more than in the case of UA STAR 197, reaching values slightly above half the reactivity of the 25P nanoparticles. For A STAR 400, the increase was also considerable since the reactivity improvement was more than three times higher than in the case of UA STAR 400. The observed differences in reactivity can be explained mainly by the characteristics of the oxide layer (**Fig. 1**).

The time required for successful activation was evaluated to be between 24 and 120 hours. **Table 2** shows that activation for longer than 48 hours has no significant influence on the reactivity of STAR 197 with Cr(VI), which has been previously observed for other ZVI samples [2, 4, 5, 7]. This increase was related to an oxide layer removal mechanism, either by dissolution [3, 6, 7] or by detachment [2, 5].

Table 2 Study of the optimal activation time for STAR 197 nanoparticles

	concentration of Cr(VI)[%]	pH	ORP [mV]
blank	100	4.9	221
Activation 0h	95.4	5.6	-13
Activation 24h	44.9	9.5	109
Activation 48h	31.4	10.3	39
Activation 72h	28.3	10.4	-46
Activation 96h	26.5	10.4	79
Activation 120h	21.7	10.5	45

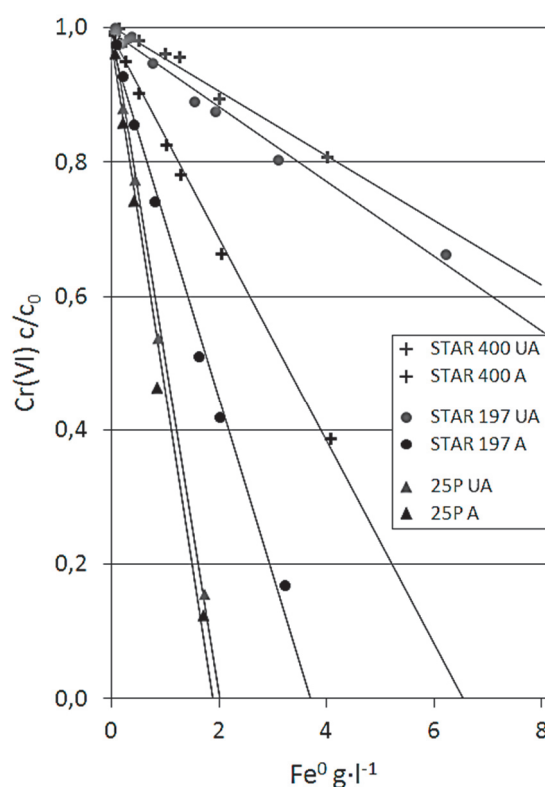


Fig. 2 Concentration tests of activated and unactivated NF 25P, STAR 400 and 197

The oxide shell protects the nZVI during storage and transport, but prior to application the activation process disintegrates this layer and opens the surface for additional treatment. In general, the reactivity and migration properties of nZVI can be improved by additional surface modification with e.g. carboxymethyl cellulose (CMC). This additive was tested on A STAR 197 (**Fig. 3**) and compared with a sample without additional modification and with UA STAR 197.

A similar decrease in Cr(VI) concentration after a reaction time of 2 hours was determined for both of the A STAR particles (with and without CMC). In the case of CMC modification, a slight prolongation of the reaction time was observed, but after 24 hours the Cr(VI) concentrations were the same for both samples. Therefore, the influence of CMC on the reaction of STAR 197 nanoparticles with Cr(VI) contamination is negligible.

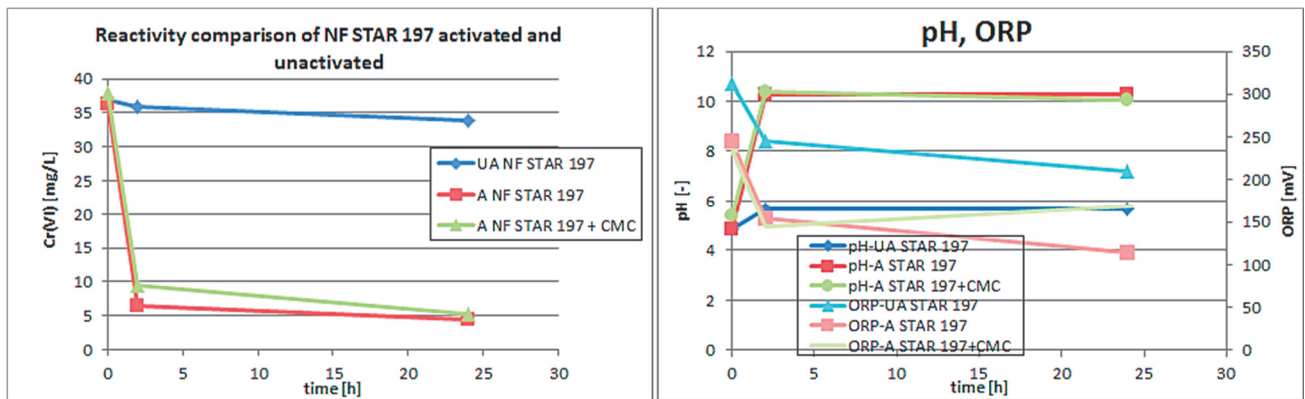


Fig. 3 Results of the batch test of STAR 197 with and without CMC treatment

Column tests

The migration properties of the activated and unactivated samples of STAR 197 and the sample modified by CMC were compared. The samples were tested in a long column (2m long, inner diameter 30 mm) with the Fe⁰ concentrations measured by magnetic susceptibility. The activation process significantly improved the migration properties of STAR 197, as shown in **Fig. 4**, where the Fe⁰ concentration (determined by frequency change) is measured through almost the whole of the column. The CMC modification worked as well as the activated nanoparticles.

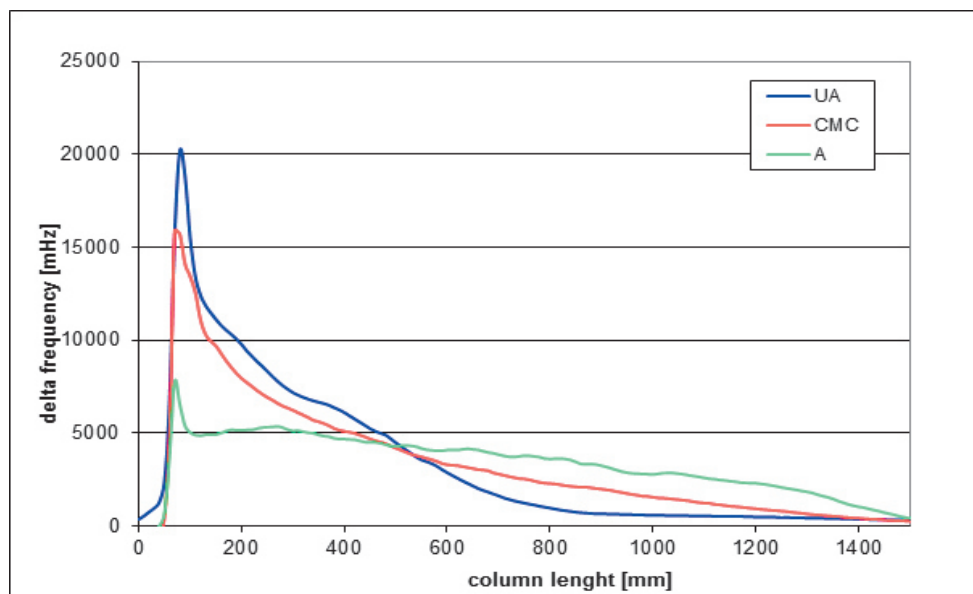


Fig. 4 Longitudinal profile of Fe⁰ in columns after 2 hours of injection for STAR 197 in different states of preparation, unactivated (UA), activated (A) and modified by CMC (CMC)

5. CONCLUSIONS

The results of the performed tests showed that the applied activation process increases the performance of surface modified nZVI particles mainly from the point of view of reactivity and migration. The process of activation leads to a breakdown and slimming down of the oxide shell allowing electron transfer without losing the appreciable quantity of ZVI (Fe^0 content). Further surface modification with CMC brought no significant improvement to the properties of the samples compared to the activation process.

ACKNOWLEDGEMENTS

The research presented in this article was supported by the project NANOREM “Taking Nanotechnological Remediation Processes from Lab Scale to End User Applications for the Restoration of a Clean Environment” under grant agreement No. 309517, the “National Programme for Sustainability I” LO 1201 and the OPR&DI project “Centre for Nanomaterials, Advanced Technologies and Innovation” CZ.1.05/2.1.00/01.0005.). The work of Kristýna Pešková was supported by the Ministry of Education of the Czech Republic within the SGS project no. 21066/115 on the Technical University of Liberec.

REFERENCES

- [1] ČERNÍK, M., a kolektiv: Chemicky podporované in situ sanační technologie, VŠCHT Praha, 2010, Czech Republic, ISBN 978-80-7080-767-5.
- [2] KIM, H. S., et al.: Atmospherically stable nanoscale zero-valent iron particles formed under controlled air contact: characteristics and reactivity. *Environmental science & technology*, 44(5), 1760-1766, 2010.
- [3] KIM, H. S., et al.: Aging characteristics and reactivity of two types of nanoscale zero-valent iron particles (Fe^0 and Fe^{II}) in nitrate reduction. *Chemical Engineering Journal*, 197, 16-23, 2012.
- [4] LIU, Y., et al.: Effect of TCE concentration and dissolved groundwater solutes on NZVI-promoted TCE dechlorination and H_2 evolution. *Environmental science & technology*, 41(22), 7881-7887, 2007.
- [5] SARATHY, V., et al.: Aging of iron nanoparticles in aqueous solution: effects on structure and reactivity. *The Journal of Physical Chemistry C*, 112(7), 2286-2293, 2008.
- [6] SOHN, K., et al.: Fe (0) nanoparticles for nitrate reduction: stability, reactivity, and transformation. *Environmental science & technology*, 40(17), 5514-5519, 2006.
- [7] XIE, Y., et al.: Influence of anionic cosolutes and pH on nanoscale zerovalent iron longevity: time scales and mechanisms of reactivity loss toward 1,1,1,2-tetrachloroethane and Cr (VI). *Environmental science & technology*, 46(15), 8365-8373, 2012.